# Variability of Cloudiness at Airline Cruise Altitudes from GASP Measurements

WILLIAM H. JASPERSON AND GREGORY D. NASTROM

*Control Data Corporation, Minneapolis, MN 55440*

RICHARD E. DAVIS

*NASA Langley Research Center, Hampton, VA 23665*

JAMES D. HOLDEMAN

*NASA Lewis Research Center, Cleveland, OH 44135*

(Manuscript received 17 March 1984, in final form 24 September 1984)

ABSTRACT

A climatology of high-altitude cloud encounters using data obtained between 1975 and 1979 from commercial airliners participating in the Global Atmospheric Sampling Program (GASP) is presented. The statistics are based on three different measures of cloudiness derived from the GASP data set. This climatology depicts the seasonal, latitudinal and altitudinal variation in the cloudiness parameters, as well as differences in the high-altitude cloud structure attributed to cyclone- and convective cloud-generation mechanisms. A qualitative agreement was found between the latitudinal distribution of cloud cover derived from the GASP data and satellite-derived high-altitude cloud statistics available in the literature. Relationships between the three different measures of cloudiness and the relative vorticity at high altitudes, stratified by season, latitude and distance from the tropopause are also presented. In midlatitudes, for example, the average cloudiness, when stratified by the sign of the relative vorticity, exhibits a seasonal cycle with the largest differences occurring in the layer 0–1.5 km below the tropopause. Seasonal and latitudinal patterns can also be seen in the other cloudiness parameters.

## 1. Introduction

The extent and variability of clouds in the atmosphere are of fundamental importance in meteorology. In recent years, Schneider (1972), Schneider *et al.* (1978), and Wetherald and Manabe (1980) among others have examined and discussed the effect and sensitivity of the feedback of cloudiness on climate variables as shown by general circulation models. Models have also shown that not only the presence of clouds but also the distribution and the optical properties of the clouds are important ingredients in their climatic effect (e.g., Herman *et al.*, 1980; Stephans and Webster, 1981; Platt and Dilley, 1981; Harshvardham, 1982). It is generally concluded that climatic increases in the amount of low and middle clouds would cause the surface temperature to decrease, while increases in the amount of high clouds would cause the surface temperature to increase.

Historically, climatologies of cloud cover have been derived from surface observations. More recently, satellites have provided an abundance of cloud data over the entire globe. Total cloud cover climatologies have been prepared (e.g., Bean and Somerville, 1981), but the difficulty of obtaining accurate cloud heights has limited work in preparing cloud climatologies by level. In a recent article, Barton (1983) utilized a differential absorption technique to determine cloud heights and amounts for clouds higher than 6 km and has presented a climatology of high clouds from two and one-half years of SCR (Selective Chopper Radiometer) data from the early 1970s. The importance of high clouds to the radiative balance problem and the uniqueness of Barton's climatology should make it very useful in many studies. Very recently, Stratospheric Aerosol and Gas Experiment (SAGE) satellite data have provided an additional source of satellite-derived high cloud data (Woodbury and McCormick, 1983).

The purpose of this paper is to present additional statistics relating to the climatology of cloud cover for altitudes above 6 km. The data were collected as a part of the Global Atmospheric Sampling Program (GASP) which used commercial aircraft in routine service as observation platforms (Perkins and Papathakas, 1977). The data recorded are thus "observations of opportunity," and even though the data were not randomly sampled in a strictly statistical sense, we believe that they do present a unique and representative climatology of cloudiness at aircraft flight

levels. Commercial aircraft deviate from great circle paths to avoid active severe weather, clear air turbulence, and restricted areas and to take advantage of wind conditions which will minimize flight times. Flight level is usually determined by aircraft weight and often is highest during the last hour or two of transcontinental flights when the fuel load is least. The avoidance of clouds, particularly the cirrus clouds which exist above 6 km, is not currently a factor in commercial aircraft flight planning. The GASP cloud observation data have an advantage over ground observation and satellite measurements in that the altitude at cloud occurrence is accurately known. Furthermore, data were collected over many times of day and even very tenuous clouds, invisible from the ground, were detected. The issue of data representativeness will be addressed further in subsequent sections. The next section describes the GASP program and data; Section 3 presents the cloud measurement statistics.

## 2. Data

The data in this study were collected as part of the NASA Global Atmospheric Sampling Program (GASP) and have been discussed in detail by Nastrom *et al.* (1981, 1982). Briefly, the data acquisition phase of GASP lasted from March 1975 to July 1979 and obtained meteorological and trace constituent data with instruments placed aboard as many as four Boeing 747 airliners in routine commercial service. Observations were recorded at nominal 5-minute intervals at all altitudes above ~6 km (20 000 ft). In addition to the basic GASP measurements, the tropopause pressure at each GASP data location has been time-and-space interpolated from the National Meteorological Center (NMC) grids, when available, and added to the archived tapes. Auxiliary meteorological data used in this study, such as vorticity, were computed for each GASP location from the NMC isobaric height fields.

The presence of clouds at aircraft altitude was determined with a light-scattering particle counter (Holdeman *et al.*, 1976). A cloud detection threshold was set based on visual observation of light haze outside the aircraft. Based on this threshold, an "in-cloud" registration resulted whenever the local aggregate particle number density (for all particles with diameters greater than 3 $\mu$m) was greater than 66 000 $m^{-3}$. Each cloud observation consisted of the number of seconds out of the preceding 256 s (4 min 16 s, or approximately 66 km at 250 m $s^{-1}$ or 500 knots ground speed) that the airplane was in-cloud.

Before proceeding, it is necessary to establish some nomenclature which will be used repeatedly in the following analyses. First, it is convenient to separate GASP observations according to whether the indicated time in clouds during the observation period was equal to, or greater than, zero. The total indicated time in clouds for an observation divided by the observation time gives the fraction of time in clouds, denoted TIC. Those observations with TIC = 0 are termed "in-clear," and those with TIC > 0 (but not necessarily equal to 100 percent) are interpreted to be in the vicinity of clouds. Next, consider a group of observations: the number of observations in the vicinity of clouds (TIC > 0) divided by the total number of observations $N$ gives the fraction of observations in the vicinity of clouds and is denoted CIV. Furthermore, the time in clouds divided by the total observation time for only those observations with TIC > 0 gives the fraction of time in clouds when in the vicinity of clouds, denoted TICIV. The time in clouds divided by the total observation time, irrespective of the presence of clouds, is denoted $\overline{\text{TIC}}$. These quantities are related by the expression:

$$\overline{\text{TIC}} = \sum_{i=1}^{N} \frac{\text{TIC}_i}{N} = \text{CIV} \times \text{TICIV}. \qquad (1)$$

Note that if the sampling interval were to approach zero seconds, then CIV would approach $\overline{\text{TIC}}$. It is assumed in this paper that TIC, the average fractional time in clouds for a group of observations, is an estimate of the average cloudiness at any given time and location in the region represented by the group of observations.

Approximately 88 000 cloud detector observations were made during the entire four-year GASP measurement period. Most of these observations came from relatively long intercontinental routes such as from the United States mainland to Hawaii or from the United States to Europe or to Japan. There also are numerous flights across the United States, between the Northern Hemisphere and the Southern Hemisphere, within the Southern Hemisphere, between cities along the southern rim of Asia, and some in Africa. A detailed summary of all flights, as well as cloud statistics and number of observations presented by altitude, latitude and longitude, can be found in Jasperson *et al.* (1984).

The distributions of the cloud observations by season, latitude, pressure–altitude, and distance from the NMC tropopause are shown in Figs. 1a–d. In each figure, a double ordinate is given. One ordinate gives the number of observations, in thousands; the other gives the percentage of observations in each category. Seasons are referenced to the Northern Hemisphere (winter = December, January, February), and the pressure-altitude is referenced to the ICAO Standard Atmosphere. (Pressure–altitude is used interchangeably with height throughout this paper.) The shaded area in each part of the figure represents the number of observations for which TIC > 0. In each case, the number above the upper (unshaded) bar represents CIV, the percentage of observations within

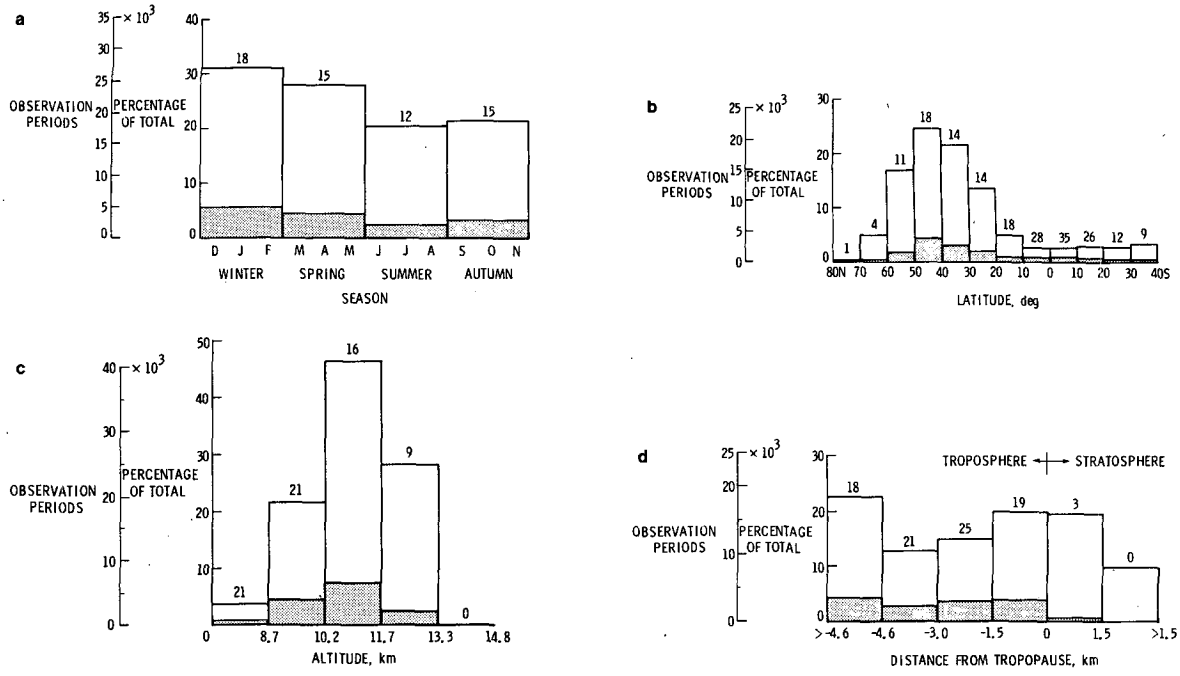


FIG. 1. Distribution of cloud detector observations by (a) season, (b) latitude, (c) altitude and (d) distance from the NMC tropopause. Shading represents observations with TIC > 0. Numbers above bars represent percentage CIV for each interval.

that bar for which TIC > 0. This latter percentage is equal to the ratio of the shaded bar to the total bar, multiplied by 100.

As shown in Fig. 1a, the number of observations is weighted slightly toward winter and spring, and a slightly higher percentage of the observations was in the vicinity of clouds in the winter than in summer. Most of the data are from the Northern Hemisphere middle latitudes, with approximately 75% of the data coming from the latitudes 20–60°N (Fig. 1b). The CIV is seen to be a maximum near the equator, with values of CIV reaching 35%. Almost 75% of the observations were made between 10.2 and 13.3 km (33.5–43.5 kft) as shown in Fig. 1c. Clouds were encountered less frequently at the higher altitudes. A stratification of the data by the distance from the NMC tropopause is presented in Fig. 1d. About 40% of the GASP observations come from within 1.5 km of the tropopause. The CIV is relatively uniform in height below the tropopause with a slight maximum in the region 1.5–3 km below it, but CIV decreases rapidly above the tropopause. The number of aircraft observations in Fig. 1d is smaller than in Fig. 1a–c (70 000) because the corresponding NMC tropopause height data were not available for some of the observations.

## 3. Results

### *a. High cloud distribution*

The GASP cloud data present a quantitative picture of the atmosphere which is consistent with phenomenological meteorological observations and global circulation models. For example, the percentage probability that an observation contains clouds in the 8.7–10.2 km pressure-altitude band is 21.2% or, equivalently, 78.8% of the observations are in clear (Fig. 2). The probability that an observation contains more than 50% cloudiness in this altitude band is 8%. In general, cloudiness above 7.6 km can be expected to decrease with height, and examination of Fig. 2 shows this to be true. Very few of the observations have cloudiness approaching 100%, which is consistent with both the patchy nature of cirrus clouds and each observation being taken over a distance of approximately 66 km.

The three cloudiness parameters averaged over all seasons and latitudes as functions of pressure–altitude are shown in Fig. 3. The average cloudiness $\overline{\text{TIC}}$ decreases with increasing height, as more and more

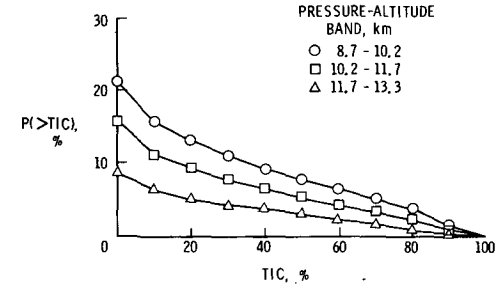


FIG. 2. Cumulative probability distribution of TIC with pressure–altitude for the entire data set.

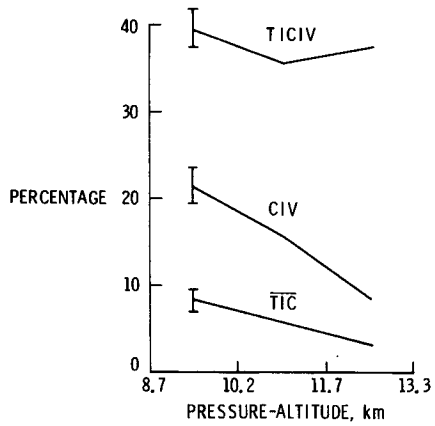


FIG. 3. Variation of mean cloudiness parameters with pressure-altitude for the entire data set.

observations come from the stratosphere. The fractional number of observations that contain at least some cloud, CIV, also decreases with increasing height. This curve indicates that clouds are spread over larger areas at lower heights and tend to be more confined in area at the higher levels. The average fractional cloudiness of those observations that contain cloud, TICIV, is seen to be relatively independent of height and to have a value of about 38%. This curve indicates that, on the average, the clouds tend to have a similar "patchy" structure at all heights, 8.7–13.3 km, even though there are more of them at the lower levels. The errors bars in the figure denote 95% confidence intervals.

The cloud data can be stratified in many ways. An analysis of variance was performed to test the statistical significance of variability in the zonal means of the cloudiness parameters $\overline{\text{TIC}}$, CIV and TICIV, resulting from change of season, latitude (30–60°N) and height (8.7–13.3 km). The results of the analysis, described in more detail in Jasperson *et al.* (1984), are summarized in Table 1. This table is a presentation of the percentage of the total variance that is explained by each variable and by the two way interactions between variables for each of the cloudiness parameters. The average cloudiness $\overline{\text{TIC}}$ is seen to vary significantly at the 99% confidence level for altitude, season and latitude; CIV shows significant variation with respect to altitude and latitude but not with respect to season. On the other hand, TICIV shows significant variation with respect to latitude and season but not with respect to altitude. This result is consistent with that shown in Fig. 3.

As discussed earlier, $\overline{\text{TIC}}$ can be interpreted as the probability of cloudiness at a point in space and time. The latitudinal distribution of $\overline{\text{TIC}}$ for three height intervals in winter and summer is presented in Fig. 4.

The winter average cloudiness, presented in Fig. 4a, shows a maximum at an average latitude of about 5°S. The relatively high values of cloudiness (14–22%) at low latitudes correspond to the presence of the Intertropical Convergence Zone (ITCZ) where the warm moist tropical air is forced upward to form large complexes of convective clouds. The highest value of cloudiness is found in the 11.7–13.3 km height band. This result is consistent with those of others (e.g., Graves, 1968) who have observed that the tropical cirrus clouds tend to be located .5 km or so below the tropical tropopause (typically 15.2–16.8 km). A minimum of 5% or less of cloudiness occurs between 15 and 25°N and corresponds to the latitudes of the subtropical high pressure belt. Cloudiness then

TABLE 1. Results of analysis of variance on the zonal means of the cloudiness parameters $\overline{\text{TIC}}$, CIV and TICIV.

| | Contribution to total variance (%) | | | Confidence level (%) | | |
|---|---|---|---|---|---|---|
| Source of variation | $\overline{\text{TIC}}$ | CIV | TICIV | $\overline{\text{TIC}}$ | CIV | TICIV |
| *Factors* | | | | | | |
| Altitude | 46.9 | 62.1 | 5.8 | 99.9 | 99.9 | 81.1 |
| Season | 15.0 | 0.7 | 25.6 | 99.9 | 17.0 | 98.8 |
| Latitude | 17.4 | 10.0 | 20.8 | 99.9 | 98.5 | 99.0 |
| All factors | 79.3 | 72.8 | 52.2 | 99.9 | 99.9 | 99.2 |
| *Two-way factor interactions* | | | | | | |
| Altitude × season | 7.8 | 2.8 | 2.4 | 97.5 | 24.8 | 5.6 |
| Altitude × latitude | 7.3 | 9.9 | 23.1 | 98.9 | 94.0 | 96.8 |
| Season × latitude | 1.3 | 4.8 | 4.2 | 30.2 | 51.9 | 17.4 |
| All two way interactions | 16.4 | 17.5 | 29.7 | 96.8 | 69.1 | 63.3 |
| *Total explained* | 95.7 | 90.3 | 81.9 | 99.9 | 99.6 | 93.7 |
| *Residual (unexplained)* | 4.3 | 9.7 | 18.1 | — | — | — |

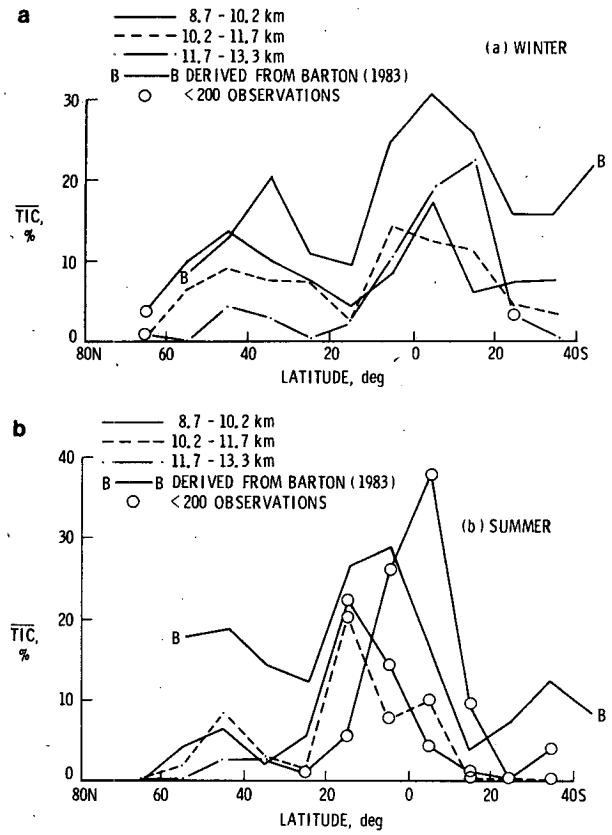


FIG. 4. Variation of average percentage of time clouds with latitude height for (a) winter and (b) summer. Symbols are plotted when there are fewer than 200 observations.

peaks again at about 45°N, caused by the presence of the traveling extratropical cyclones. In midlatitudes, the average cloudiness is largest in the lowest altitude band; this is caused by the upper two altitude bands usually being in the stratosphere at these latitudes.

The summer average cloudiness, presented in Fig. 4b, basically shows a similar pattern. The equatorial peak, at least for the lowest two altitude bands, has followed the seasonal migration of the ITCZ northward and is located at about 15°N. The peak at the equator is based on only 40–60 observations, not all of which are independent, while most of the curves in Fig. 4 are based on hundreds to thousands of observations. The minimum cloudiness has also moved northward to 25–35°N. The midlatitude peak is again at about 45°N but has a much smaller amplitude. This is believed to be a reflection of the different nature of the cirrus-producing systems between winter and summer, with thunderstorms dominating the summertime production and fronts and cyclones dominating the wintertime production.

Figures 4a, b represent zonal means of average cloudiness. Cloud encounter climatologies gridded by latitude, longitude, height (as well as distance from the tropopause), and season can be found in Jasperson *et al.* (1984). It is apparent from these climatologies that there are longitudinal differences in cloudiness. It is also acknowledged that the GASP flights did not uniformly sample all longitudes. There is a legitimate question about how well the GASP data represents the latitudinal structure. To address this question, we have compared our results to those of Barton (1983). In his study, Barton used a differential absorption technique with two and one-half years of data from the Nimbus 5 SCR to obtain a climatology of clouds above 6 km. His curves of percent cloud cover for seasonal zonal means are denoted by B in Fig. 4. In general, Barton's curves indicate a higher level of cloudiness than the GASP curves. This is consistent with the observational fact that high clouds, when present at one level, are not necessarily present at all levels. Nevertheless, the correspondence in the shape between Barton's data and the GASP data is striking. The largest percentage difference occurs during midlatitude summers and may be partially due to the fact that Barton's curve corresponds to clouds at local noon, a time when summertime convective activity might begin. Short and Wallace (1980) have shown that there is a substantial diurnal variation in cloudiness, even at high levels.

The variation of the cloudiness parameters with respect to pressure–altitude and season for all data between 40 and 50°N is shown in Fig. 5. The plots of $\overline{\text{TIC}}$ and CIV with altitude for each season are similar to their overall global plots in Fig. 3, except

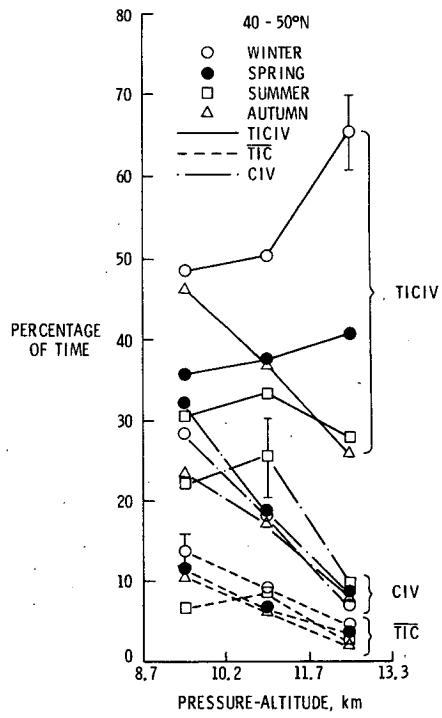


FIG. 5. Variation of cloudiness parameters with pressure–altitude by season at 40–50°N latitude.

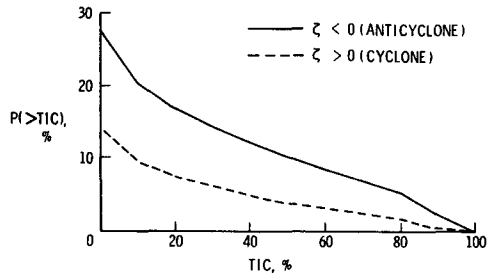


FIG. 6. Cumulative probability distribution of TIC 0–3 km below the tropopause in cyclones and anticyclones.

for the summer season, which shows a peak in each plot at the middle altitude level. Although this peak does not appear to be highly significant as seen by the 95% confidence intervals, it may be an indication of more wide spread high-altitude cloudiness in summer, resulting from many separate thunderstorm sources. The TICIV is relatively constant with respect to height in spring and summer but varies markedly in autumn and winter. The decrease with height in autumn may be due to the seasonal transition between summer and winter; autumn is associated with relatively few intense thunderstorms or well-developed cyclones which produce high-level cloudiness in these latitudes. In contrast, TICIV in winter increases markedly with height. Even though there are relatively few clouds at the highest level (small $\overline{\text{TIC}}$), the clouds when present cover substantial areas. This curve may reflect the presence of occasional, very well developed winter cyclones which generate substantial cirrus coverage.

### *b. High clouds and vorticity*

We will now present the results of stratifying the GASP cloud data by the algebraic sign of the relative vorticity. As shown in Fig. 6, there is a strong dependence between the sign of the relative vorticity and cloudiness. Note that more clouds are associated with anticyclonic vorticity than with cyclonic vorticity at flight levels 8.7–13.3 km, consistent with Bergeron's classical three-dimensional cloud and circulation model of a cyclone (Byers, 1959).

The $\overline{\text{TIC}}$ for latitudes 30–70°N are presented for each season in Fig. 7. The largest differences of $\overline{\text{TIC}}$

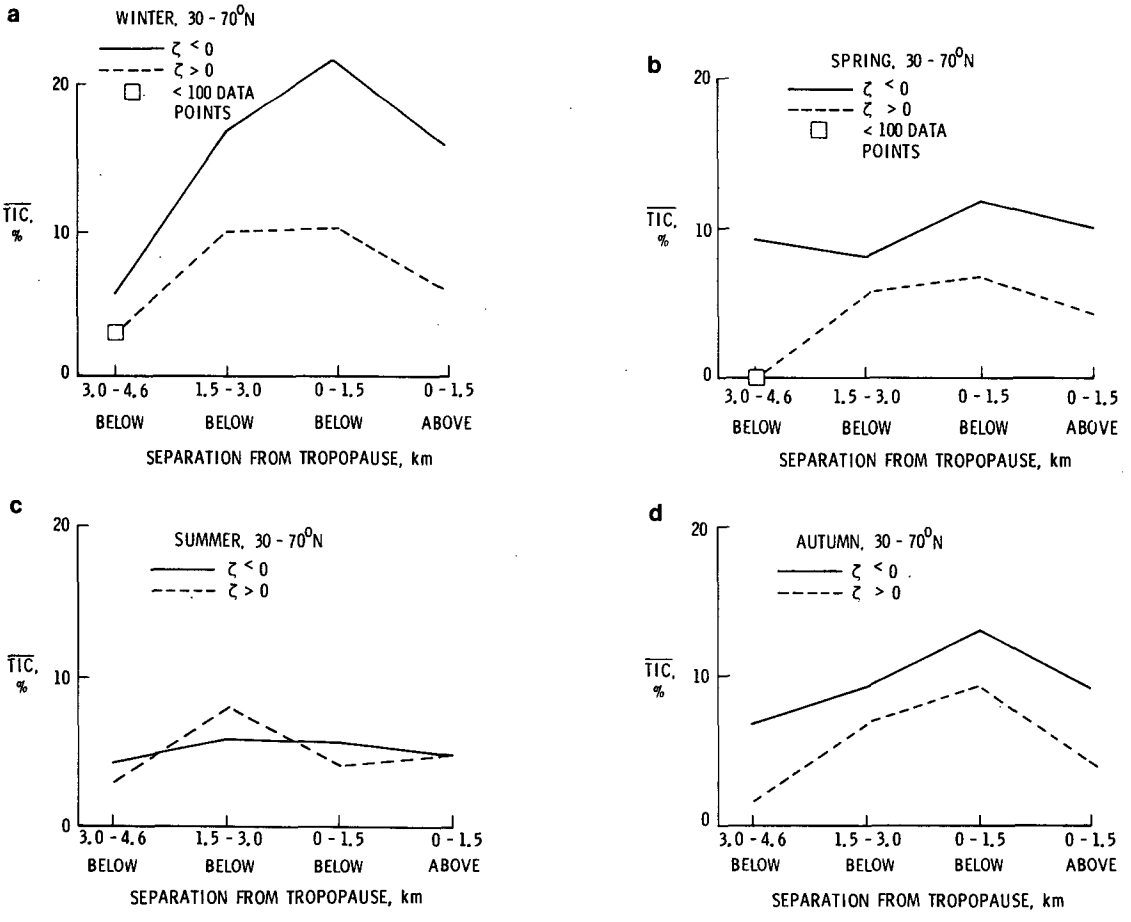


FIG. 7. Variation of TIC in cyclones and anticyclones as a function of distance from the NMC tropopause in (a) winter, (b) spring, (c) summer and (d) autumn.

between positive and negative relative vorticity occur in winter, and the largest value for each season occurs in the 1.5 km layer immediately below the tropopause. During summer $\overline{TIC}$ is near 5%, independent of the vorticity and distance from the tropopause. This picture is consistent with the seasonal model of fewer and weaker cyclones in summer with relatively more of the high clouds produced from convective storms. The spring and autumn $\overline{TIC}$ exhibit behavior representative of transition periods between winter and summer.

The probability of cloud encounter, CIV, as a function of vorticity and distance from the tropopause, latitude, and season (summer and winter) is presented in Fig. 8. The difference in the mean values of CIV for positive and negative relative vorticity situations is greatest in the winter and for heights near the tropopause. Positive relative vorticity and clouds are positively correlated in the lower atmosphere; this is consistent with the crossing of the curves at 3.0–4.6 km below the tropopause in winter. Also during winter, the maximum value of CIV occurs 0–1.5 km below the tropopause when the relative vorticity is negative and 3.0–4.5 km below the tropopause when it is positive. As observed with TIC, the values are much smaller in summer than in winter, particularly with negative vorticity. Another feature shown in Fig. 8 is that the values of CIV are smaller for latitudes 30–40°N than for higher latitudes. This is true in both seasons and for both signs of the relative vorticity.

In Fig. 9, we present TICIV as a function of the sign of vorticity and distance from the tropopause, latitude, and season (winter and summer). In winter, TICIV is almost always larger at all heights when the relative vorticity is negative. The maximum value consistently occurs 0–1.5 km below the tropopause. Note that TICIV decreases very rapidly in winter as the distance below the tropopause increases. However, no obvious pattern is visible in the summer.

### *c. Independence of high cloud observations*

The question of data independence must be addressed on different scales. At the largest scale, the concern is with either the presence or absence of clouds in an observation. Given one of these conditions, how many observations later is the probability of the condition reoccurring equal to the population probability? Assuming that the population probability can be approximated by the overall sample probability, the answer was found to be about 18 observations, or 90 min of flight time. This corresponds to 1400 km (865 statute miles) at a 500-knot ground speed. There is only a slight tendency for this number to increase with height between 8.7 and 13.3 km.

On a smaller scale, one can pose a second question: given that a cloud is present (TIC > 0), how many observations must be skipped before the value of TIC is independent of the first value? The answer to this question varies with the value of TIC. When TIC was less than 50%, observations separated by 10–20 min were found to be independent. When TIC was greater

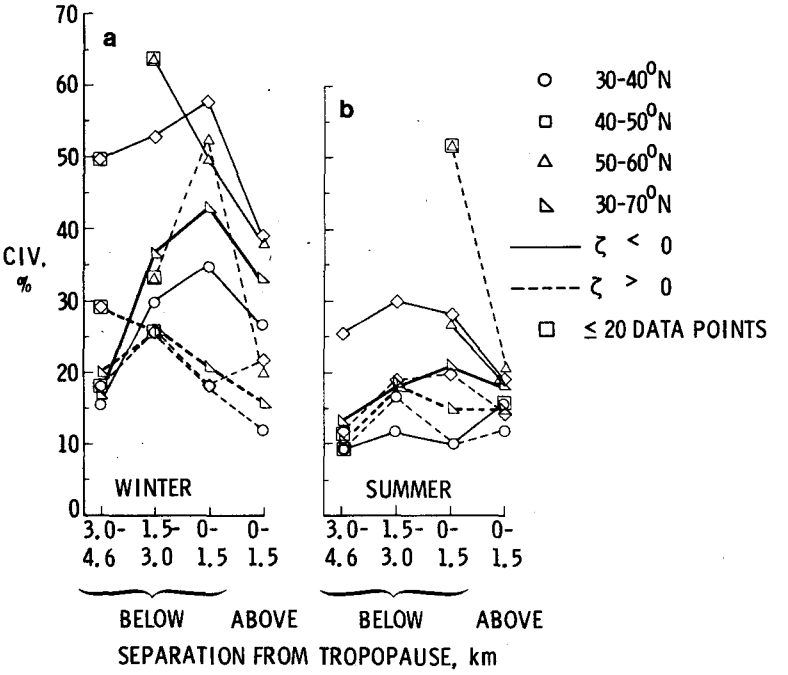


FIG. 8. Variation of CIV as a function of distance from the NMC tropopause, by latitude and sign of vorticity in (a) winter and (b) summer.

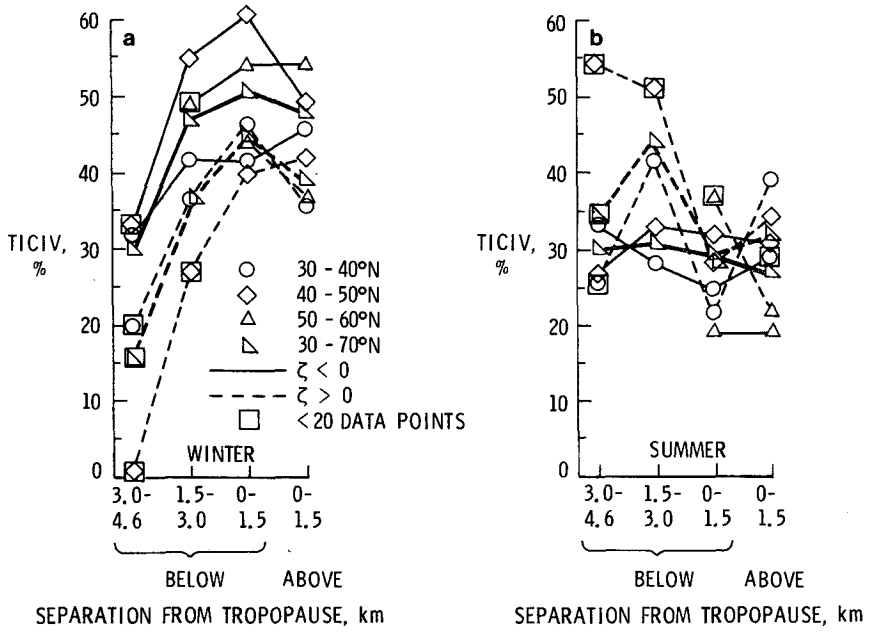


FIG. 9. Variation of TICIV as a function of distance from the NMC tropopause by latitude and sign of relative vorticity in (a) winter and (b) summer.

than 50%, the time between independent observations increased to over one hour, the longest time that could be estimated from the GASP data.

The analysis of independence illustrates the organization of clouds in the atmosphere. Once an aircraft encounters a cloud (TIC > 0), the likelihood that TIC will remain greater than zero for many tens of minutes is high. The value of TIC, however, will tend to vary substantially over periods of minutes. The higher the value of TIC, the more likely it is that the value will remain high for longer periods of time. These characteristics are not unexpected, but the specific results serve to quantify an atmospheric variable previously described only qualitatively. Finally, these results were used to estimate the number of independent observations in constructing error bars such as those used in Figs. 3 and 5.

## 4. Summary

The GASP cloud data set provides useful information on cloudiness at aircraft flight levels. The GASP cloudiness climatology closely resembles the high cloud distribution presented by Barton (1983). The climatology depicts the seasonal variation in cloudiness as well as differences in the structure of the high-level clouds due to differences in the generating sources (cyclones versus convective storms).

The relationships between cloudiness and the relative vorticity computed from the NMC analysis fields are also presented. The average area percentage of clouds shows a seasonal dependence with a maximum in winter in the interval 0–1.5 km below the tropopause. Minimum cloudiness is found in summer with no differences observed between positive or negative relative vorticity. The CIV and TICIV also show seasonal differences as well as differences with respect to distance from the tropopause and latitude.

The characteristics of cloudiness apparent in the analysis of data independence is also consistent with meteorological observation. The horizontal extent of the cloudiness is larger when clouds are present over a substantial portion of a cloud observation. Independence between observations on this large scale occurs after distances of 1000 km or more. When cloudiness is present over many small portions of the cloud observation, data are independent after only 150–300 km.

## REFERENCES

Barton, I. J., 1983: Upper level cloud climatology from an orbiting satellite. *J. Atmos. Sci.*, **40**, 435–447.

Bean, S. J., and P. N. Somerville, 1981: Some new worldwide cloud cover models. *J. Appl. Meteor.*, **20**, 223–228.

Byers, H. R., 1959: *General Meteorology.* McGraw-Hill, 540 pp.

Graves, M. E., 1968: Aircraft reports of cirriform clouds on certain high-latitude routes and California to Honolulu. *Mon. Wea. Rev.*, **96**, 809–812.

Harshvardham, 1982: The effect of brokenness on cloud–climate sensitivity. *J. Atmos. Sci.*, **39**, 1853–1861.

Herman, G. F., M.-L. C. Wu and W. T. Johnson, 1980: The effect of clouds on the earth's solar and infrared radiation budgets. *J. Atmos. Sci.*, **37**, 1251–1261.

Holdeman, J. D., F. M. Humenik and E. A. Lezberg, 1976: NASA global atmospheric sampling program (GASP) data report for

tape VL0004. NASA TM X-73574, NASA Lewis Research Center, Cleveland, OH, 47 pp. [NTIS N77-13563.]

Jasperson, W. H., G. D. Nastrom, R. E. Davis and J. D. Holdeman, 1984: GASP cloud- and particle-encounter statistics and their application to LFC aircraft studies. NASA TM-85835, NASA Langley Research Center, Hampton, VA. Vol. 1, 90 pp. [NTIS N84-34828.] Vol. 2, 212 pp. [NTIS N85-12522.]

Nastrom, G. D., J. D. Holdeman and R. E. Davis, 1981: Cloud-encounter and particle-concentration variabilities from GASP data. NASA TP-1886, NASA Langley Research Center, Hampton, VA, 244 pp. [NTIS N82-15677.]

——, —— and ——, 1982: Cloud encounter and particle number density variabilities from GASP data. *J. Aircr.*, **19,** 272–277.

Perkins, P. J., and L. C. Papathakos, 1977: Global sensing of gaseous and aerosol trace species using automated instrumentation on 747 airliners. NASA TM-73810, NASA Lewis Research Center, Cleveland OH, 11 pp. [NTIS N78-13670.]

Platt, C. M. R., and A. C. Dilley, 1981: Remote sounding of high clouds. Part IV: Observed temperature variations in cirrus optical properties. *J. Atmos. Sci.*, **38,** 1069–1082.

Schneider, S. H., 1972: Cloudiness as a global feedback mechanism: The effects on radiation balance and surface temperature of variations in cloudiness. *J. Atmos. Sci.*, **29,** 1413–1422.

——, W. H. Washington and R. M. Chervin, 1978: Cloudiness as a climatic feedback mechanism: Effects on cloud amounts of prescribed global and regional surface temperature changes in the NCAR GCM. *J. Atmos. Sci.*, **35,** 2207–2221.

Short, D. A., and J. M. Wallace, 1980: Satellite-inferred morning-to-evening cloudiness changes. *Mon. Wea. Rev.*, **108,** 1160–1169.

Stephans, G. L., and P. J. Webster, 1981: Clouds and climate: Sensitivity of simple systems. *J. Atmos. Sci.*, **38,** 235–247.

Wetherald, R. T., and S. Manabe, 1980: Cloud cover and climate sensitivity. *J. Atmos. Sci.*, **37,** 1485–1510.

Woodbury, G. E., and M. P. McCormick, 1983: Global distributions of cirrus clouds determined from SAGE data. *Geophys. Res. Lett.*, **10,** 1180–1183.